Surface & Coatings Technology 231 (2013) 117–121

Contents lists available at ScienceDirect

Surface & Coatings Technology

journal homepage: www.elsevier.com/locate/surfcoat

Improvement in the bias stability of amorphous InGaZnO TFTs using an Al_2O_3 passivation layer

Sheng-Yao Huang [a], Ting-Chang Chang [a,b,*], Min-Chen Chen [a], Te-Chih Chen [a], Fu-Yen Jian [c], Yu-Chun Chen [a], Hui-Chun Huang [d], Der-Shin Gan [d]

[a] Department of Physics, National Sun Yat-Sen University, Kaohsiung, 804, Taiwan, ROC
[b] Center for Nanoscience & Nanotechnology, National Sun Yat-Sen University, Kaohsiung, 804, Taiwan, ROC
[c] Department of Electronics Engineering, National Chiao Tung University, Hsinchu, 300, Taiwan, ROC
[d] Department of Materials and Optoelectronic Science, National Sun Yat-Sen University, Kaohsiung, 804, Taiwan, ROC

ARTICLE INFO

Available online 8 January 2012

Keywords:
Thin film transistors
Indium gallium zinc oxide
Passivation
Bias stress

ABSTRACT

This work presents the light–color-dependent negative bias stress (NBIS) effect on amorphous indium gallium zinc oxide (a-IGZO) thin film transistors (TFTs) with Al_2O_3 passivation layer. The colors of incident photon are varied from red to blue, that incident photon energies are all lower than the optical band gap of IGZO (3.2 eV). The experimental results show that the Al_2O_3 passivated devices present stable electrical behaviors under different incident lights (ΔV_T<0.1 V of dark and red, ΔV_T<1 V of green, and ΔV_T<4 V of blue), whereas the unpassivation devices exhibit observable negative shifts during NBIS (ΔV_T<1 V of dark and red, ΔV_T>8 V of green, andΔV_T>15 V of blue). The degradation mechanism of the negative bias stress under illumination of a-IGZO TFTs is dominated by the photo-generated hole trapping at the gate insulator and/or interface between insulator and channel. In this result, the Al_2O_3 passivation layer can effectively passivate the defect in the a-IGZO film, reducing electron hole pair generated during the illumination processed.

1. Introduction

Recently, active-matrix organic light-emitting diode (AMOLED) displays have attracted much attention due to their superior performances, such as wide viewing angle, fast response time, high luminance brightness, and contrast ratio [1–3]. To achieve such products, thin film transistors (TFTs) are one of the key building blocks in the circuitry to control the pixel elements. Transparent oxide-base TFTs, such as amorphous indium–gallium–zinc oxide (a-IGZO) TFTs, have been regarded as suitable devices for active driving OLED displays because they offer higher (electron) mobility (>10 cm^2/Vs) than that of amorphous silicon (a-Si) TFTs. At the same time, they have excellent uniformity compared with polycrystalline silicon (poly-Si) TFTs, good optical transparency (>80%) in visible light region, and low deposition temperature [4–11]. In addition, a-IGZO has also been extended to as a nonvolatile memory [12,13]. There is a promising integration of a-IGZO TFT arrays on the same glass substrate for advanced system-on-panel (SOP) applications.

To be display backplane electronics, it is crucial for a-IGZO TFTs to exhibit bias independent reliability and stability when exposure to the illumination. However, it has been demonstrated that the device characteristics of oxide TFTs were influenced by the adsorption/desorption of gas molecules from ambient onto the exposed back-channel surface [14,15]. Therefore, the passivation is helpful to obtain a stable a-IGZO TFTs. In our previous study, the Al_2O_3 layer has a good passivation ability to suppress gas absorption, especially for H_2O absorption [16]. However, the impact of the Al_2O_3 passivation layer for light illumination has not been thoroughly studied, and is worthy for further investigation. Therefore, we examine the stability under light illumination or in the dark, and discuss the mechanism for devices with and without an Al_2O_3 passivation layer in this study.

2. Experiment

The bottom gate coplanar a-IGZO TFTs were produced on glass substrate in this study, and the fabrication details were described elsewhere [16]. The schematic cross-section view and of the TFTs is shown in Fig. 1(a). Briefly, the shaped Ti/Al/Ti (50/200/50 nm) gate electrodes were capped with 300-nm-thick SiO_x gate dielectric. The source/drain electrodes were formed with DC-sputtered Ti/Al/Ti (50/200/50 nm) and then patterned into the dimension of channel width/length (W/L)= 10–15 μm/9 μm by wet-etching. A 30-nm-thick a-IGZO thin film was deposited as active layer by DC magnetron sputtering system using a target of In:Ga:Zn=1:1:1 in atomic ratio. After defining the active region by conventional photolithography, the devices were annealed in an oven at 330 °C for 2 h. Finally, the passivated device was capped with 30 nm thick Al_2O_3 film by RF sputtering at room temperature, and annealed again at 330 °C for 2 h to reduce the ion bombardment effect during the sputtering process [17]. The TFTs without any passivation were

* Corresponding author at: Department of Physics, National Sun Yat-Sen University, Kaohsiung, 804, Taiwan, ROC. Tel.: +886 7 5252000 3708; fax: +886 7 5253709.
E-mail address: tcchang@mail.phys.nsysu.edu.tw (T.-C. Chang).

0257-8972/$ – see front matter.
doi:10.1016/j.surfcoat.2011.12.047

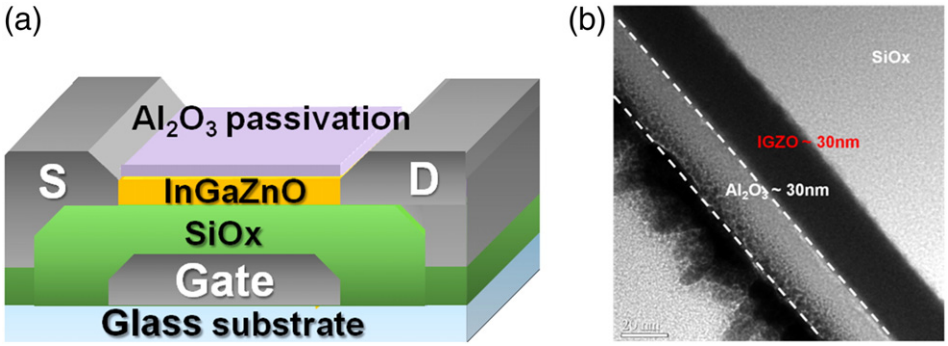

Fig. 1. (a) The cross-section schematic view of the fabricated a-IGZO TFT structure. (b) The cross-sectional TEM imaged of the a-IGZO thin film.

taken as reference devices for comparison. Fig. 1(b) also shows the cross-sectional transmission electron microscopy (TEM) image of the TFT device. The laminated structure of the Al_2O_3/IGZO/SiO_x in the TEM image can easily be observed. The IGZO film is uniform without any observable microstructure, indicating that the IGZO layer is amorphous in structure although it was heated up to 330 °C during annealing. The electrical characteristics of the TFTs were analyzed by using Agilent B1500 system in the dark environment and measured in a vacuum chamber, a pressure of 10^{-3} Torr to avoid the disturbance from atmosphere. The linear mobility was extracted by normal method of the square root normalized drain current ($NI_D = I_D \times L/W$) verse gate voltage (V_G) plot, and the threshold voltage (V_{th}) is defined as the V_G of the NI_D reaching 1 nA. The sub-threshold slope (SS) was extracted from NI_D in the sub-threshold region (the NI_D from 1^{-10} A to 10^{-8} A) under linear operation.

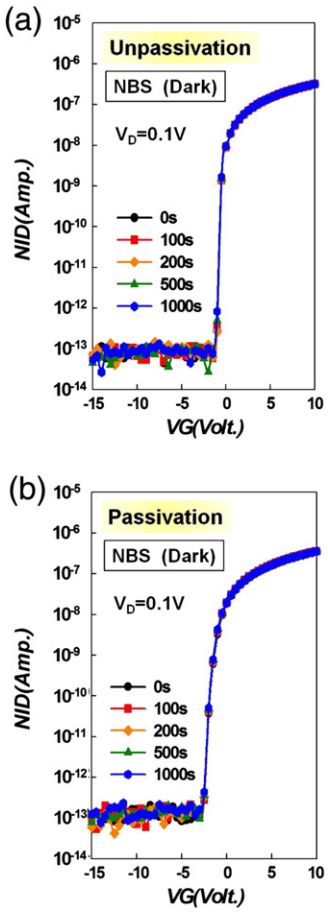

Fig. 2. Transfer characteristics for the (a) unpassivated (device A) and (b) passivatied (device B) device during the negative bias stress (NBS) in dark.

3. Results and discussion

Fig. 2 (a) and (b) shows the transfer characteristics of the a-IGZO TFT for the unpassivated (device A) and passivated (device B) device during negative bias stress in dark (NBS), respectively. For the stress condition, the gate voltage was fixed at the V_G of −30 V and the S/D electrodes were grounded. In the initial electrical properties, the device A exhibits the SS = 0.17 V/dec, field-effect mobility (u) = 11.65 cm^2/Vs, and V_{th} = −0.6 V. The device B also shows excellent electrical properties, such as the SS = 0.34 V/dec, field-effect mobility (u) = 11.14 cm^2/Vs, and V_{th} = −1.3 V. Both of the devices with similar $I_{on/off}$ ratios of 10^8 are observed. It indicates that a-IGZO film is not degraded during the passivation Al_2O_3 layer deposition by sputtering. In addition, both of the devices show superior stabilities, without degradation of SS, on current, and obvious V_{th} shift during NBS.

In order to study the instability under light illumination and discuss the illuminated mechanism for devices with and without an Al_2O_3 passivation layer, the devices expose in different wavelength illumination were investigated. Fig. 3 shows the spectra of LEDs, including red (photo-energy 1.93 eV), green (photo-energy 2.35 eV), and blue (photo-energy 2.64 eV) lights. All employed light sources in this study possess a sub-bandgap (a-IGZO). Fig. 4(a) and (b) show the corresponding V_{th} variations of device A and B in the I_D–V_G curves, respectively, which are subjected to various colored illumination stresses (IS) without applying bias. The IS conditions are $V_G = V_D = Vs = 0$ V, and the light intensity under illumination is 8000 lx for 1000 s. In device A, blue and green lights have negative threshold voltage shifts smaller than 5 V, but the electrical properties are stable in the red light illumination. Compared with device A, device B is stable in all the wavelength light illumination, which slight threshold voltage shift is smaller than 0.5 V. The obvious V_{th} variations of device A during the blue and the green IS can be attributed to the O_2 desorption in the back channel of a-IGZO bulk. Fig. 5(a) and (b) exhibits the schematic mechanisms for the proposed

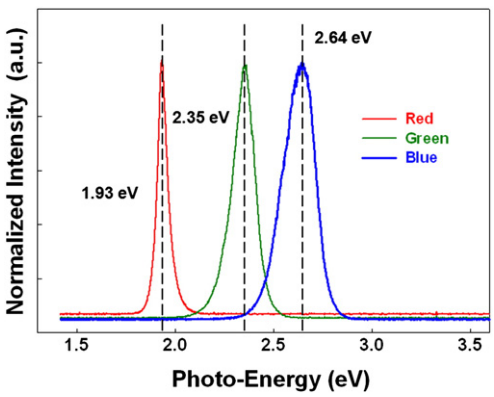

Fig. 3. The spectrum of the employed LEDs for red, green, blue light.

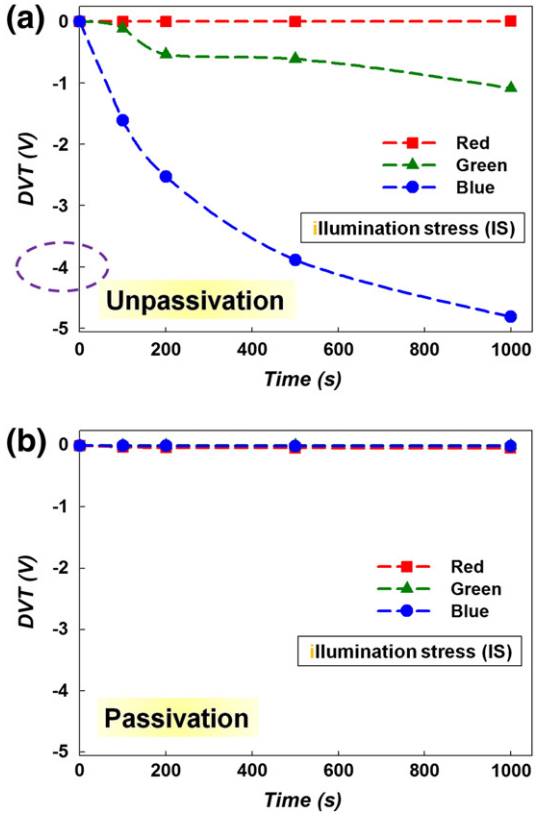

Fig. 4. The light illuminated time dependence of V_{th} shift during various colored illumination stress (IS) without applying bias for (a) unpassivation (device A) and (b) passivated (device B) device.

O_2 desorption model under light illumination for devices A and B, respectively. Since the O_2 adsorbed on the a-IGZO film, which can capture electrons in the back channel exists as O^{2-} in a form of $O_2 + e^- \rightarrow O_2^-$, leading to a decrease of the carrier concentration of a-IGZO film and an increase in V_{th} [14,15,18,19]. However, under light illumination, the holes generated from light inducing electron–hole pairs react with the absorbed O_2^- to reduce into O_2 in the back channel, resulting in a negative V_{th} shift. In addition, the blue light IS shows a larger negative V_{th} shift than other wavelength lights (red and green), because the high photo-energy of blue light induces the more absorbed O_{2-} to reduce into O_2 in the back channel. In contrast, the device B with Al_2O_3 passivation can suppress the gas adsorption/desorption in the back channel of a-IGZO film, resulting in that the electrical property shows a more stability ($\Delta V_{th} < 0.5$ V) during the all wavelength light IS.

Moreover, the negative bias illumination stress (NBIS) induced instability of the electrical properties was investigated in the study. In the stress condition, the gate voltage was fixed at the V_G of −30 V and the S/D electrodes were grounded in different wavelength light (red, green, blue) illumination for 1000 s. Fig. 6(a), (b) and (c) shows the I_D–V_G characteristics for devices A during NBIS in different wavelength lights (red, green and blue). Fig. 6(a) shows the I_D–V_G characteristics of device A during negative bias red (photo-energy is 1.93 eV) illumination stress. Device A exhibits only a slight negative V_{th} shift without other degradation during negative bias red light illumination stress (NBRIS). During the negative bias green light (photo-energy is 2.35 eV) illumination stress (NBGIS), a large negative V_{th} shift more than NBRIS is present, as shown in Fig. 6(b). Compared with NBRIS and NBGIS, device A exhibits a significant large photo leakage current during the negative bias blue light (photo-energy is 2.64 eV) illumination stress (NBBIS), which induces a larger negative V_{th} shift more than 15 V and a poor gate control on the channel current, as shown in Fig. 6(c). This result indicates that the tendency of V_{th} shift increases gradually as the light photo-energy increases during NBIS for device A. In contrast to device A, the I–V characteristics of device B during NBIS in different wavelength lights (red, green, and blue) show a superior stability, which the V_{th} slightly shifts ($\Delta V_{th} < 4$ V) toward negative direction without degradation of SS. The V_{th} shift also increases gradually as the light photo-energy increases during NBIS.

Fig. 7(a) shows the schematic models of subgap DOS in a-IGZO. The high density of occupied subgap states near the valence band with an energy width of ~1.5 eV as reported by Nomura et al. [20,21]. Fig. 7(b) exhibits the energy band of the a-IGZO TFT under NBIS. The subgap photon excitation can occur from the deep-subgap DOS to the conduction band under illumination when illumination light provides enough photo-energy (>1.7 eV), resulting in free electron concentration increases in the a-IGZO film [22]. Moreover, a negative bias is applied with illumination, resulting in the hole trapping in the insulator or a-IGZO/insulator interface [23,24]. Both of the results induce the apparent V_{th} shift under NBIS. The short wavelength of illumination light has more photo-energy than long wavelength, which induces more free electron concentration and hole trapping. This result exhibits that the V_{th} shift also increases gradually as the light photo-energy increases during NBIS. Compared to NBIS, the devices (devices A and B) show a superior stability without V_{th} shift during NBS. The lack of apparent V_{th} variation under NBS can

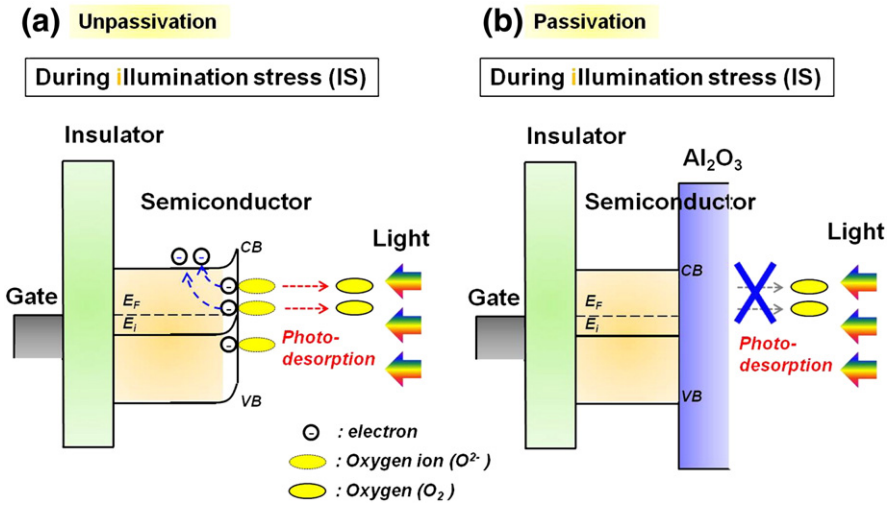

Fig. 5. Energy band diagrams of the O_2 desorption mechanism under light illumination for (a) unpassivation (device A) and (b) passivation (device B) device.

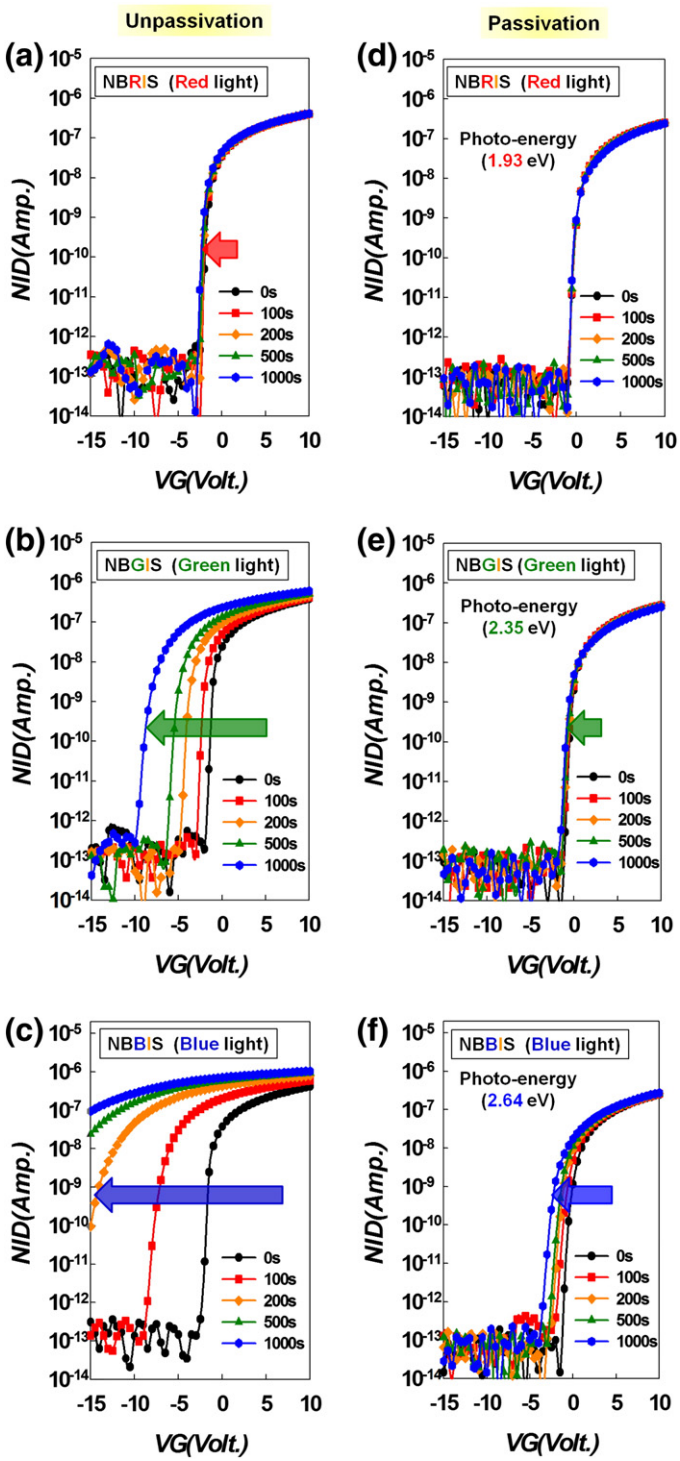

Fig. 6. Transfer I–V characteristics for the unpassivation (device A) during the negative bias illumination stress (NBIS) of (a) red, (b) green, and (c) blue lights. Transfer I–V characteristics for the passivation (device B) during the negative bias illumination stress (NBIS) of (d) red, (e) green, and (f) blue lights.

be attributed to the negligible holes in the n-type ZnO-based material [25,26]. Therefore, the hole trapping at either the gate insulator or at the a-IGZO interface can be ignored. However, the Al_2O_3 passivation device (device B) shows a slighter V_{th} shift (ΔV_{th}<4 V) than the device A during NBIS, because the Al_2O_3 passivation layer decreases the deep-subgap density that induces the photo-excitation behavior decrease. Hence, the Al_2O_3 is an effective passivation layer to suppress the photo-excitation on a-IGZO film that enhances the illumination stability and negative bias light illumination stability.

4. Conclusion

In conclusion, the Al_2O_3 passivation layer enhancing the illumination stable was investigated. The Al_2O_3 passivation layer suppresses the gas adsorption/desorption in the back channel of a-IGZO film. It induces the electrical property that shows a more stability (ΔV_{th}<0.5 V) during all wavelength lights IS. In contrast, no passivation device shows a larger negative V_{th} shift than Al_2O_3 passivation device because the holes generated form light inducing electron–hole pairs react with

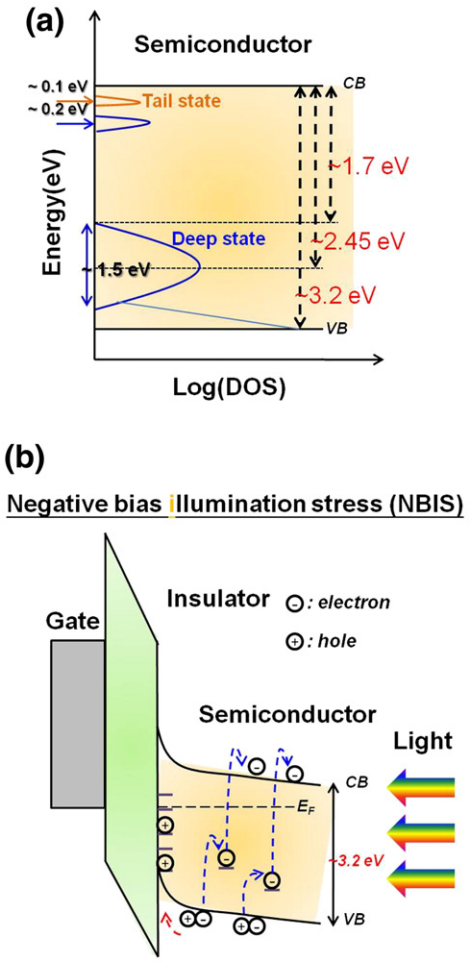

Fig. 7. (a) Schematic model of subgap DOS in a-IGZO TFTs. (b) Energy band diagram of explain the negative bias illumination stress instability.

the absorbed O_2^- to reduce into O_2 under illumination. Otherwise, the negative bias illumination stress induced instability of the electrical properties was investigated in the study. The subgap photon excitation occurs from the deep-subgap DOS inducing that the hole generates and traps in the insulator or IGZO/insulator interface under NBIS, resulting in the apparent negative V_{th} shift. However, the Al_2O_3 passivation device exhibits a slighter V_{th} negative shift ($\Delta V_{th}<4$ V) than the no passivation device under NBIS due to the decrease of hole trapping. The hole trap decreases because the Al_2O_3 passivation layer decreases the deep-subgap density that results in the photo-excitation behavior decrease. In addition, Hence, Al_2O_3 is an effective passivation layer to suppress gas absorption on InGaZnO back channel and decrease photo-excitation behavior.

Acknowledgment

This work was performed at the National Science Council Core Facilities Laboratory for Nano-Science and Nano-Technology in Kaohsiung-Pingtung area and was supported by the National Science Council of the Republic of China under Contract Nos. NSC 100-2120-M-110-003.

References

[1] M. Stewart, R.S. Howell, L. Pires, M.K. Hatalis, W. Howard, O. Parche, IEDM Tech. Dig. (1998) 871.
[2] R.M.A. Dawson, Z. Shen, D.A. Furest, S. Connor, J. Hsu, M.G. Kane, R.G. Stewart, A. Ipri, C.N. King, P.J. Green, R.T. Flegal, S. Pearson, C.W. Tang, S. Van Slyke, F. Chen, J. Shi, M.H. Lu, J.C. Sturm, IEDM Tech. Dig. (1998) 875.
[3] H.Y. Lu, P.T. Liu, T.C. Chang, S. Chi, IEEE Electron Device Lett. 27 (2006) 743.
[4] T.C. Chen, T.C. Chang, T.Y. Hsieh, W.S. Lu, F.Y. Jian, C.T. Tsai, S.Y. Huang, C.S. Lin, Appl. Phys. Lett. 99 (2011) 022104.
[5] J.S. Park, T.W. Kim, D. Stryakhilev, J.S. Lee, S.G. An, Y.S. Pyo, D.B. Lee, Y.G. Mo, D.U. Jin, H.K. Chung, Appl. Phys. Lett. 95 (2009) 013503.
[6] Y.C. Chen, T.C. Chang, H.W. Li, S.C. Chen, J. Lu, W.F. Chung, Y.H. Tai, T.Y. Tseng, Appl. Phys. Lett. 96 (2010) 262104.
[7] C.T. Tsai, T.C. Chang, S.C. Chen, I. Lo, S.W. Tsao, M.C. Hung, J.J. Chang, C.Y. Wu, C.Y. Huang, Appl. Phys. Lett. 96 (2010) 242105.
[8] H. Kumomi, K. Nomura, T. Kamiya, H. Hosono, Thin Solid Films 516 (2008) 1516.
[9] W.F. Chung, T.C. Chang, H.W. Li, S.C. Chen, Y.C. Chen, T.Y. Tseng, Y.H. Tai, Electrochem. Solid-State Lett. 14 (6) (2011) H235.
[10] M.C. Chen, T.C. Chang, S.Y. Huang, K.C. Chang, H.W. Li, S.C. Chen, J. Lu, Y. Shi, Appl. Phys. Lett. 94 (2009) 162111.
[11] K.H. Ji, J.-I. Kim, Y.-G. Mo, J.H. Jeong, S. Yang, C.-S. Hwang, S.-H.K. Park, M.-K. Ryu, S.-Y. Lee, J.K. Jeong, IEEE Electron Device Lett. 31 (2010) 1404.
[12] M.C. Chen, T.C. Chang, S.Y. Huang, S.C. Chen, C.W. Hu, C.T. Tsai, Simon M. Sze, Electrochem. Solid-State Lett. 13 (6) (2010) H191.
[13] M.C. Chen, T.C. Chang, C.T. Tsai, S.Y. Huang, S.C. Chen, C.W. Hu, S.M. Sze, M.J. Tsai, Appl. Phys. Lett. 96 (2010) 262110.
[14] D. Kang, H. Lim, C. Kim, I. Song, J. Park, Y. Park, J.G. Chung, Appl. Phys. Lett. 90 (2007) 192101.
[15] J.S. Park, J.K. Jeong, H.J. Chung, Y.G. Mo, H.D. Kim, Appl. Phys. Lett. 92 (2008) 072104.
[16] S.Y. Huang, T.C. Chang, M.C. Chen, S.C. Chen, C.T. Tsai, M.C. Hung, C.H. Tu, C.H. Chen, J.J. Chang, W.L. Liau, Electrochem. Solid-State Lett. 14 (4) (2011) H177.
[17] J. Park, S. Kim, C. Kim, S. Kim, I. Song, H. Yin, K.-K. Kim, S. Lee, K. Hong, J. Lee, J. Jung, E. Lee, K.-W. Kwon, Y. Park, Appl. Phys. Lett. 93 (2008) 053505.
[18] J.K. Jeong, H.W. Yang, J.H. Jeong, Y.G. Mo, H.D. Kim, Appl. Phys. Lett. 93 (2008) 123508.
[19] T.C. Chen, T.C. Chang, T.Y. Hsieh, C.T. Tsai, S.C. Chen, C.S. Lin, M.C. Hung, C.H. Tu, J.J. Chang, P.L. Chen, Appl. Phys. Lett. 97 (2010) 192103.
[20] K. Nomura, T. Kamiya, H. Yanagi, E. Ikenaga, K. Yang, K. Kobayashi, M. Hirano, Hosono, Appl. Phys. Lett. 92 (2008) 202117.
[21] H. Oh, S. Mi . Yoon, M.K. Ryu, C.S. Hwang, S. Yang, S.H.K. Park, Appl. Phys. Lett. 97 (2010) 183502.
[22] K.-H. Lee, J.S. Jung, K.S. Son, J.S. Park, T.S. Kim, R. Choi, J.K. Jeong, J.-Y. Kwon, B. Koo, S. Lee, Appl. Phys. Lett. 95 (2009) 232106.
[23] P. Görrn, M. Lehnhardt, T. Riedl, W. Kowalsky, Appl. Phys. Lett. 91 (2007) 193504.
[24] J.H. Shin, J.S. Lee, C.S. Hwang, S.H.K. Park, W.S. Cheong, M. Ryu, C.W. Byun, J.I. Lee, H.Y. Chu, ETRI J. 31 (2009) 62.
[25] A. Suresh, J.F. Muth, Appl. Phys. Lett. 92 (2008) 033502.
[26] M.E. Lopes, H.L. Gomes, M.C.R. Medeiros, P. Barquinha, L. Pereira, E. Fortunato, R. Martins, I. Ferreira, Appl. Phys. Lett. 95 (2009) 063502.